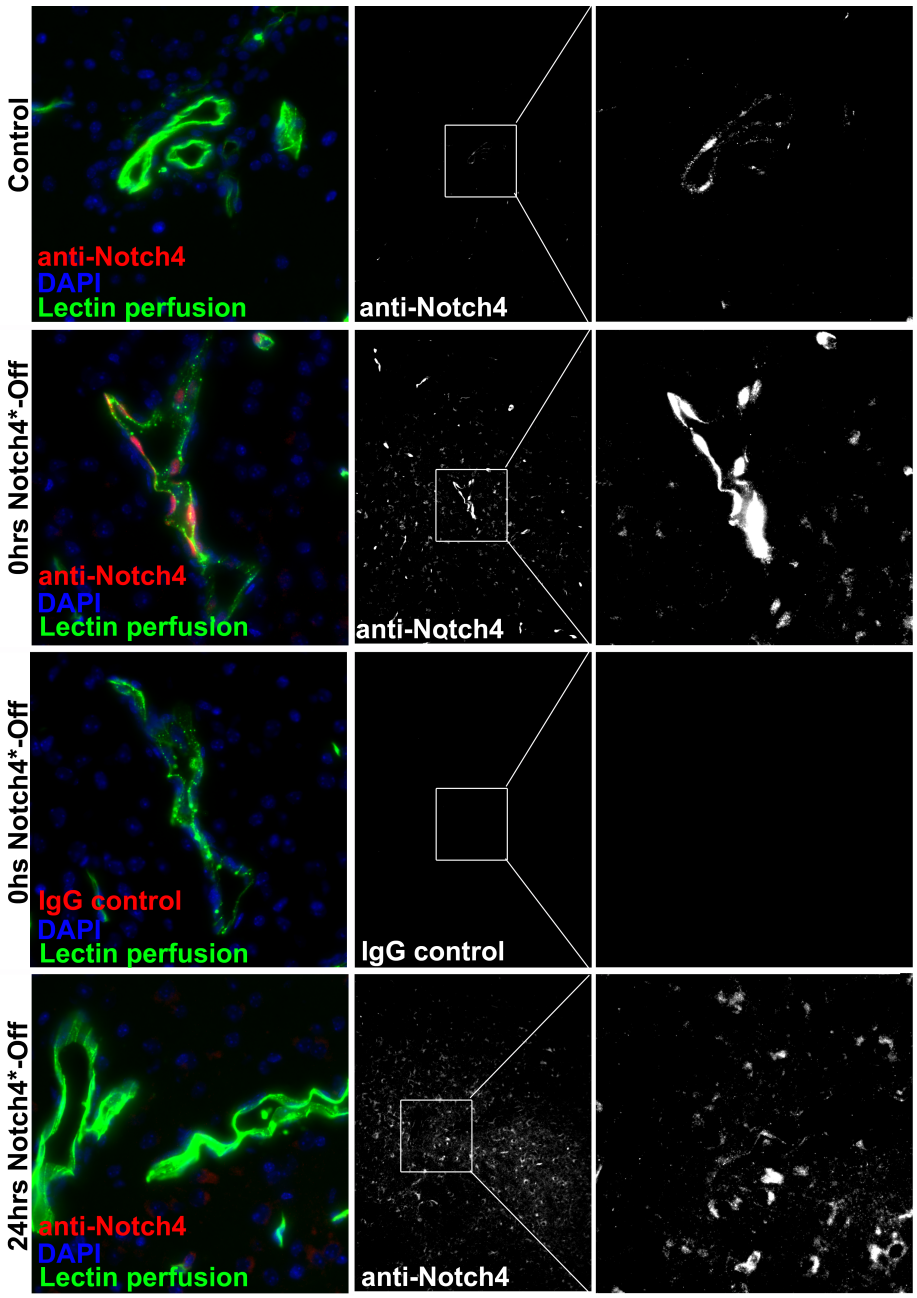

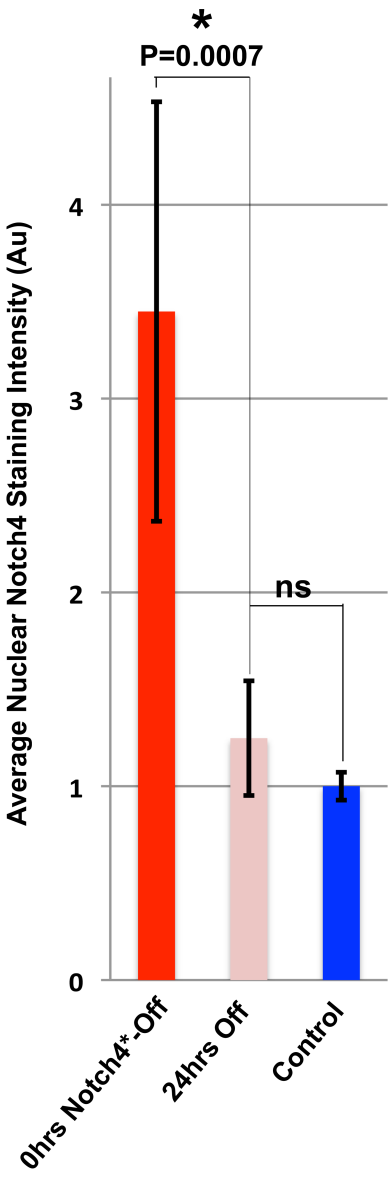

Figure S1. *Notch4 repression occurs within 24hrs of doxycycline treatment**

Frozen sagittal brain sections with fluorescent immunostaining for Notch4 intracellular domain, with labeling of perfused vessels by tomato lectin staining, and nuclear labeling by DAPI. Images show overlap of Notch4 stain with DAPI in cells lining lectin-perfused vessels. Isolation and amplification of the Notch4 staining shows light Notch4 signal in the control vessel nuclei, strong expression in the vessels of mutants before *Notch4** suppression (0hrs *Notch4**-Off), and light expression after 24hrs doxycycline treatment (24hrs *Notch4**-Off). Graph shows quantification of fluorescent intensity in endothelial cell nuclei of brain vasculature in *Notch4** mutants before and after Dox treatment, and their littermate controls. Error bars represent s.d. between individual animals (n=6 at 0hrs *Notch4**-Off, n=6 at 24hrs *Notch4**-Off, and n=6 controls). In each animal, three nuclei in each of three vessels were quantified to yield an average intensity. *P=0.0007.

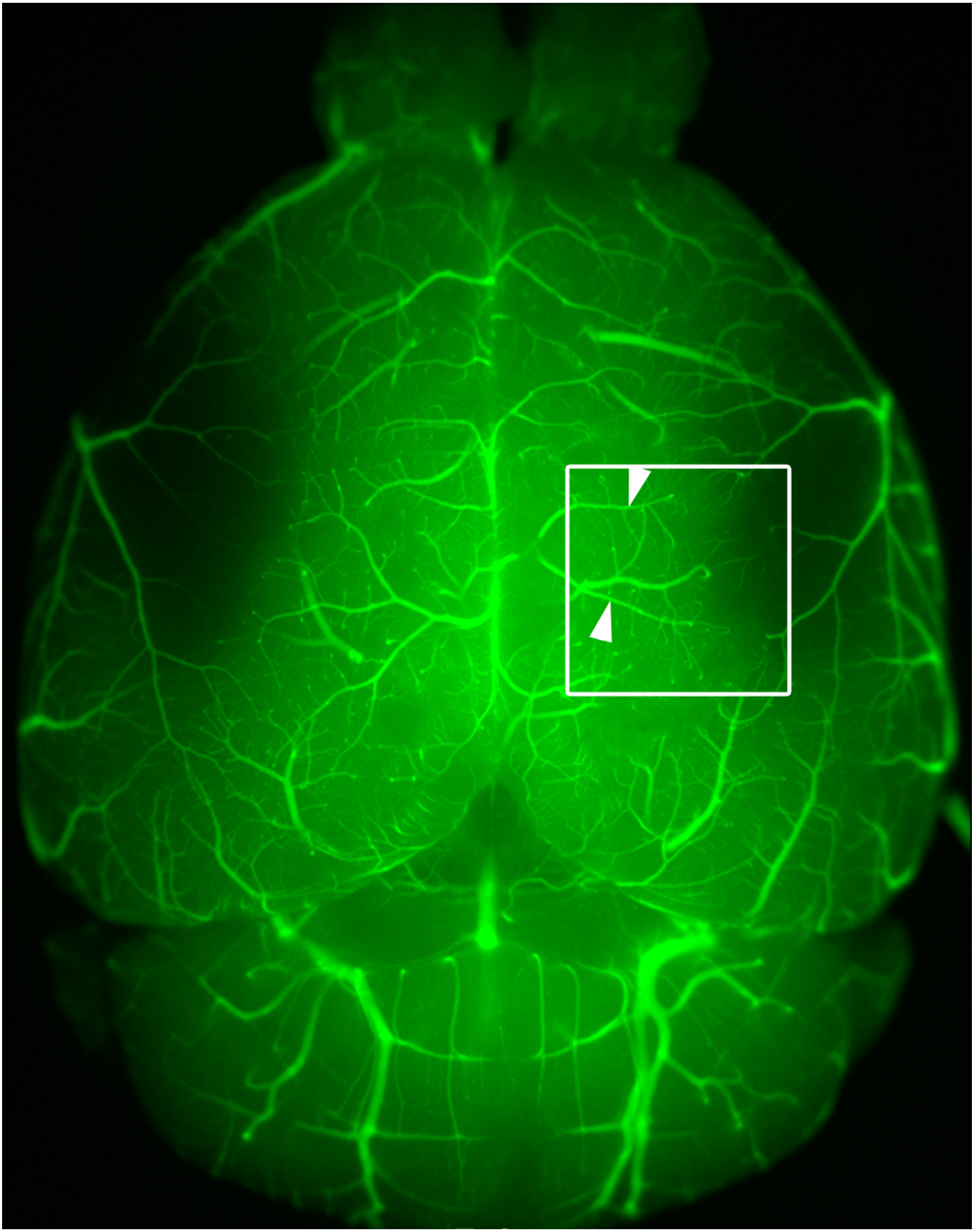

Figure S2. Placement of the chronic imaging window
Perfusion of the whole brain with fluorescein-labeled agarose shows pial arteries (arrowheads) and the typical placement of the window (boxed area).

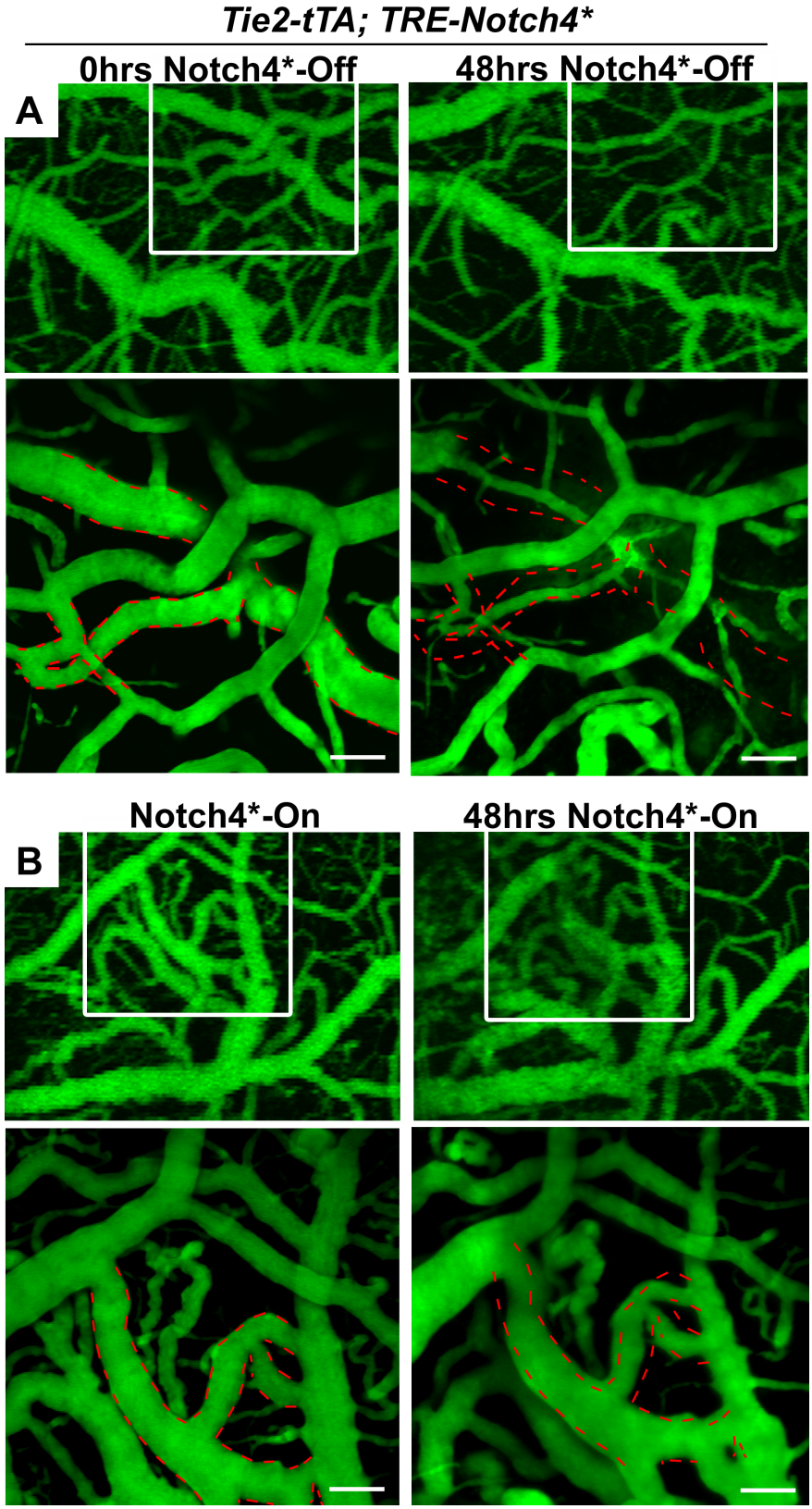

Figure S3. Specific regression of AV shunts after repression of *Notch4** Two-photon timelapse imaging of cortical brain vessels through cranial window in *Notch4** mutant mice. Plasma labeling was provided by intravenous FITC-dextran. (A) Regression of existing AV shunts following 48hrs of *Notch4** repression (B) Regression did not occur without *Notch4** repression. Note the reduction in the size of the distal vessels to the enlarging AV shunt in B. Scale bars = 100μm.

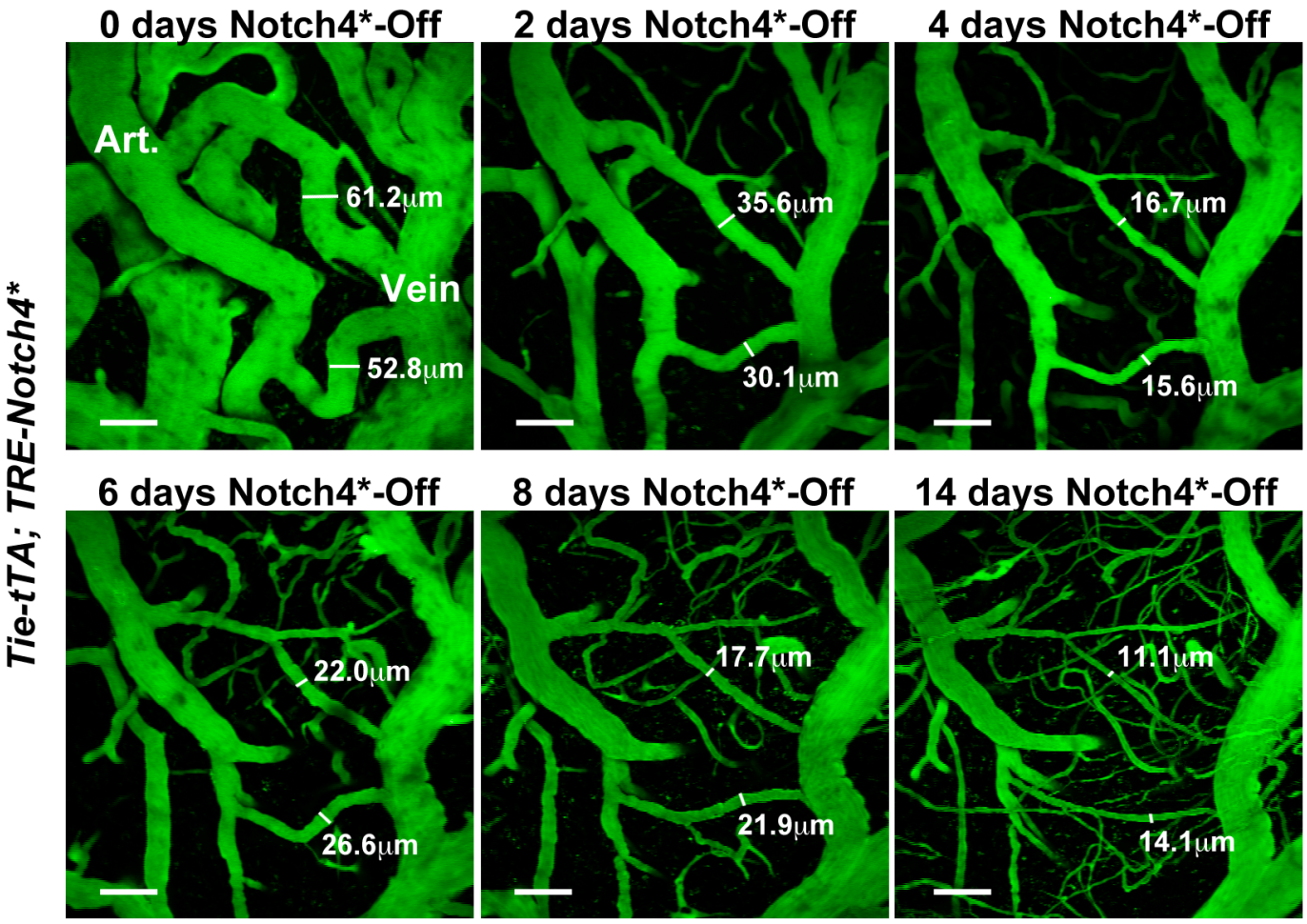

Figure S4. Repression of Notch4* induces regression of well-established large AV malformation
Two-photon timelapse imaging of cortical brain vessels in Notch4* mutant mice after well-established AV malformation. Vessel topology was visualized by intravenous FITC-dextran. Windows were placed on mice demonstrating ataxic symptoms, corresponding with advanced-stage disease. The diameters of large AV shunts were reduced following repression of Notch4* (n = 20 AV shunts in 3 mice). The majority of regression occurred rapidly within the first week and continued to two weeks. Detection of FITC-dextran-perfused capillaries adjacent to AV malformations increases over time. Scale bars = 100μm.

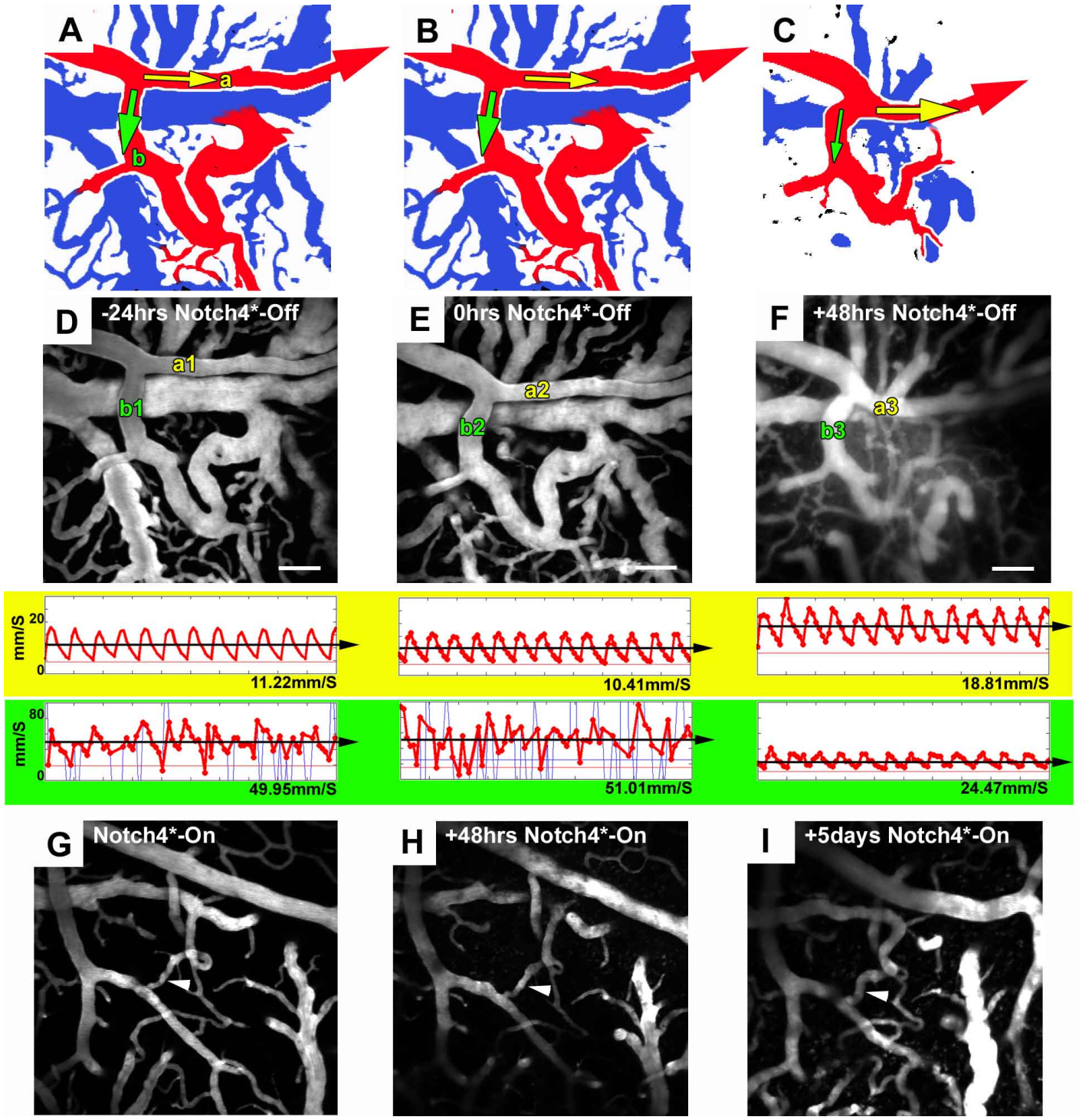

Figure S5. AV shunts are stable until repression of *Notch4

(A-C) Color-coded depiction of the AV shunt imaged by two-photon timelapse imaging in (D-F), arteries are in red and veins are in blue. AV shunt remained for 24 hours without repression of *Notch4** (Compare D and E), but regressed with 48hrs of *Notch4** repression (Compare E and F). Bottom panels show velocity traces obtained by line scan in the vessels indicated by yellow or green arrows (A-C). Velocity in AV shunt feeding artery (green) decreased, while velocity in the non-AV shunt artery increased (yellow), during regression of the AV shunt. (G-I) Without treatment, AV shunts continue to grow (arrowheads in G-H). Figure is representative of results in 10 AV shunts in 8 mice for Notch4*-Off and 5 AV shunts in 2 mice for Notch4*-On. Scale bars = 100μm.

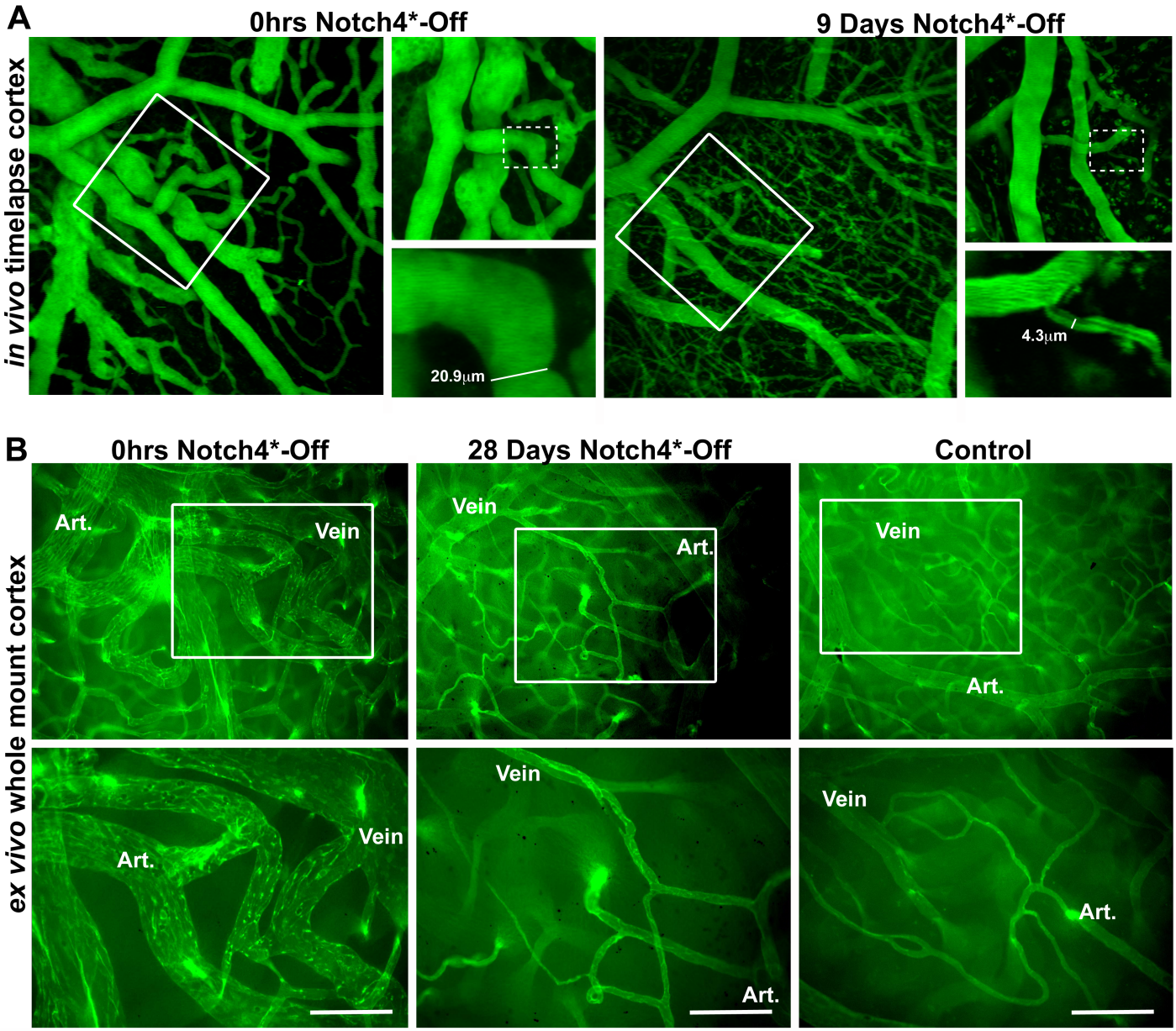

Figure S6. AV shunts regress to capillary diameter vessels in mice with and without cranial window
(A) Two-photon timelapse imaging of cortical brain vessels through cranial window in *Notch4** mutant mouse. Plasma labeling was provided by intravenous FITC-dextran. Large AV shunt regressed to capillary diameter within 9 days of *Notch4** repression. (B) *Ex vivo* imaging of whole mount cortex from mice perfused with FITC-lectin. Prior to *Notch4** repression, large AV shunts were observed between artery and vein. In a similarly affected littermate mutant, following 28 days of *Notch4** repression, AV connections were reduced to the diameter of capillaries in littermate control mice. *n*=3 mutants before *Notch4**-Off , *n*=5 littermate mutants after *Notch4**-Off, *n*=5 controls. Scale bars = 100μm

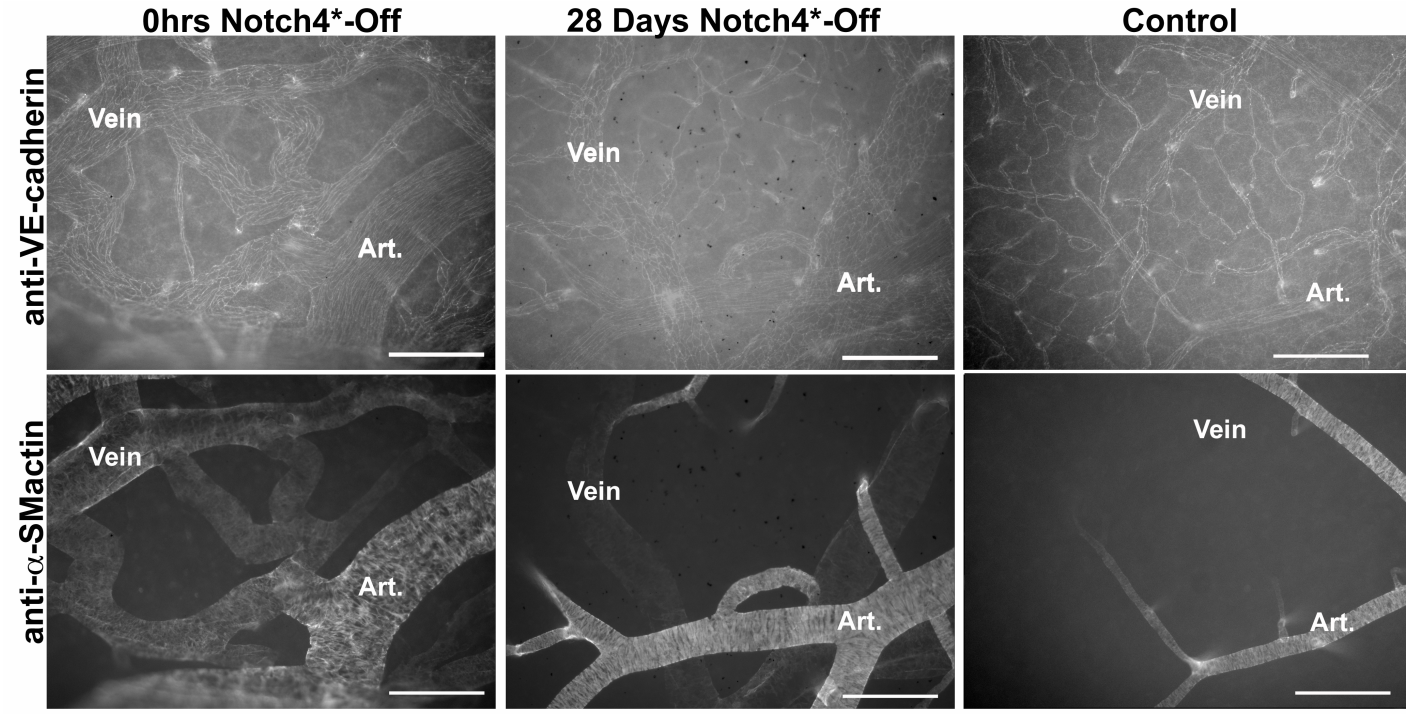

Figure S7. Smooth muscle coverage is normalized by suppression of Notch4*.
Whole mount immuno-staining of cerebral cortex. VE-cadherin staining shows vasculature and outline of individual ECs. α-Smooth muscle actin staining shows smooth muscle cell coverage and alignment. Note the reduction in smooth muscle cell coverage in the vein after repression of Notch4*, relative to the littermate mutant before Notch4* repression. *n*=3 mutants before *Notch4**-Off , *n*=5 littermate mutants after *Notch4**-Off, *n*=5 controls. Scale bars = 200μm.

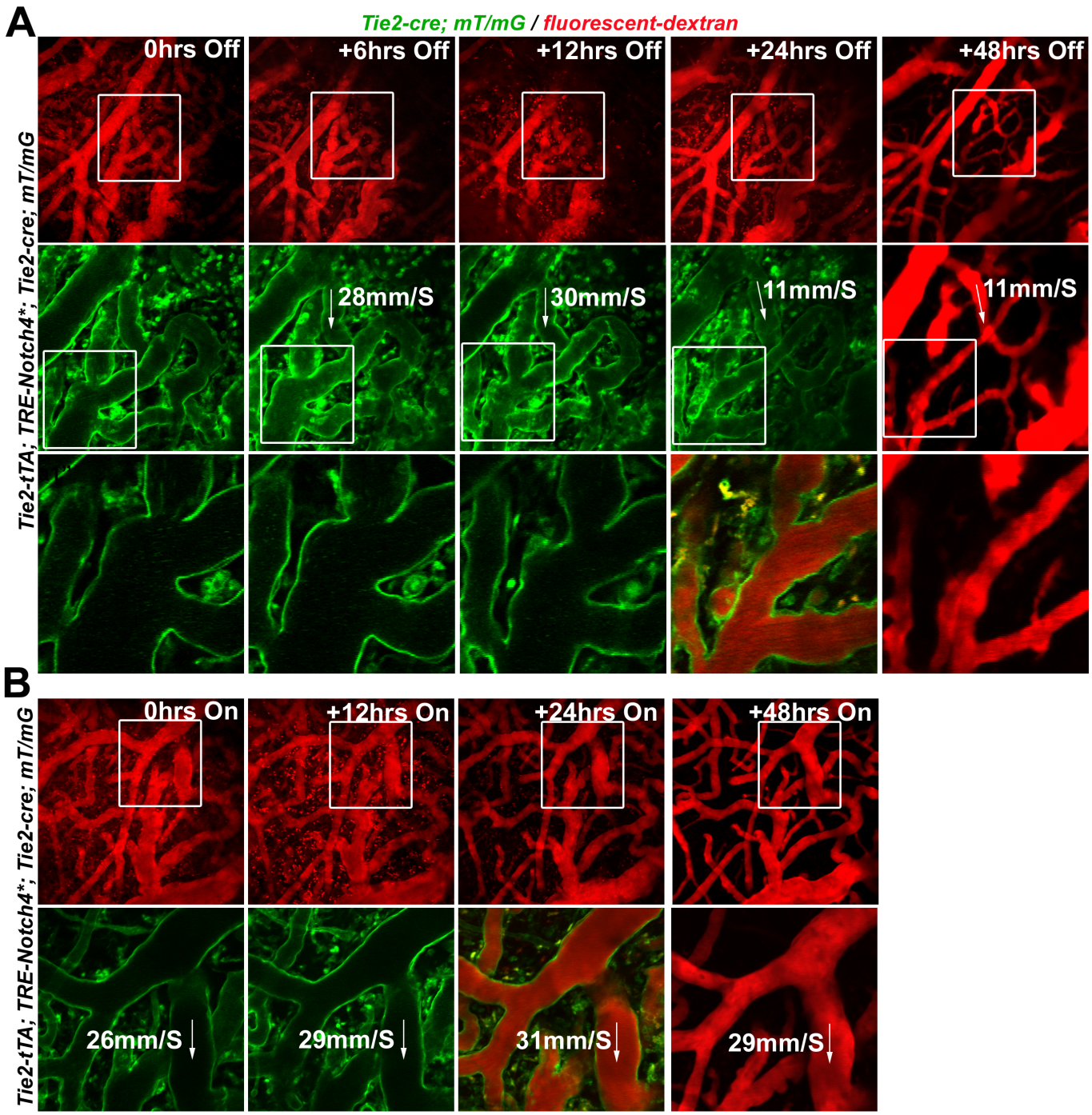

Figure S8. Velocity changes coincide with narrowing of AV shunts and distal vein beginning by 12-24hrs after *Notch4 repression**

In vivo timelapse imaging of *Tie2-tTA; TRE-Notch4*; Tie2-cre; mT/mG* mice (green endothelial fluorescence), with TRITC-dextran labeling of plasma (red). (A) With repression of *Notch4**, AV shunt regression began between 12 and 24hrs, coinciding with a reduction in blood velocity through the AV shunt. (B) Without repression of *Notch4**, AV shunt diameter and velocity were maintained. Note the reduction of distal vessel size. Blood flow was measured in this distal vessel, and was reduced over time.

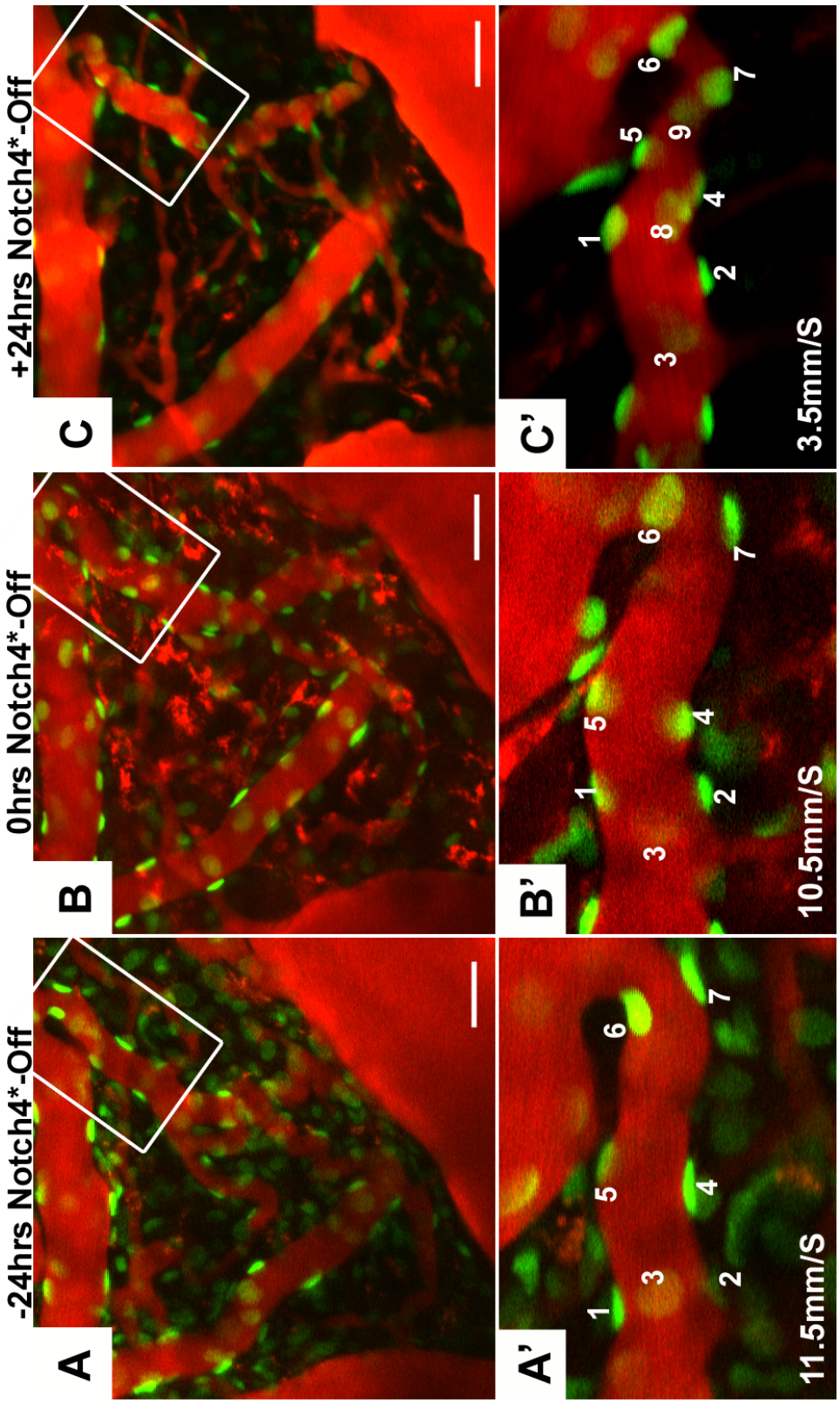

Figure S9. Narrowing of ephrinB2-GFP+ AV shunt occurs specifically after *Notch4 repression**
(A-C) Two-photon time-lapse imaging through a cranial window following repression of *Notch4** in *Tie2-tTA; TRE-Notch4*; ephrinB2*$^{+/H2B\text{-}eGFP}$ mutant with labeling of plasma by Texas-Red dextran. An AV shunt showed little change in diameter or centerline velocity (bottom left corner) after 24hrs without repression of *Notch4** (B). Within 24hrs of *Notch4** repression (C), the AV shunt was greatly reduced in diameter, with a reduction in blood velocity. Note that the same number of cells were present, but grouped closer. Scale bars = 100μm.

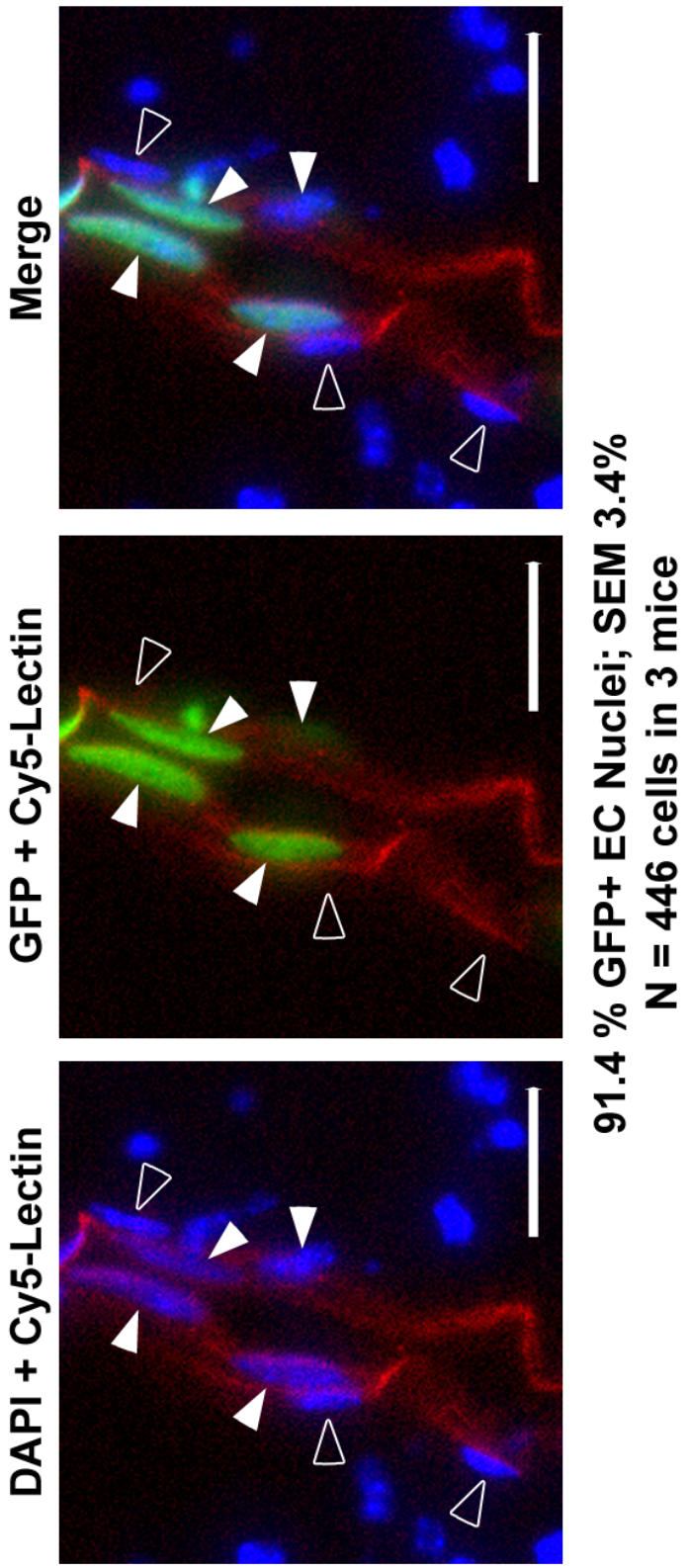

Figure S10. ***Tie2-tTA; TRE-H2B-eGFP*** **marks brain endothelial cells.**
Imaging of GFP+ endothelial cells from sectioned brain specimens of *Tie2-tTA; TRE-GFP*; *TRE-Notch4** mice perfused with Cy5 bound tomato-lectin. Endothelial nuclei were identified by co-localization of DAPI staining and Cy5 signal in cells along the wall of patent vessel lumens. Nuclei fully enveloped by Cy5 signal were considered endothelial cells (closed arrow heads) and other vascular cells were not (open arrow heads). Triple-color merged image showing DAPI, GFP+ nuclei, and Cy5-labeled endothelium. Two-color merged imaged showing GFP+ nuclei and Cy5-labeled endothelium. Scale bars = 20μm. Quantification of GFP+ endothelial cells from 446 analyzed nuclei in 3 mice.

A

% of Starting Diameter	Time after Notch4* Repression				
	0hrs	12hrs	20hrs	28hrs	36hrs
n=100%	38	2	1		
90≤n<100%		9	1		
80≤n<90%		13	8		
70≤n<80%		10	11	6	1
60≤n<70%		3	7	12	10
50≤n<60%		1	4	11	11
40≤n<50%			4	5	8
30≤n<40%			1	3	6
20≤n<30%			1	1	2

Diameter %	100	85.9	69.2	57.7	51.0
s.e.m %		0.9	4.0	3.0	2.9

B

% Cells Remaining in AV Shunt	Time after Notch4* Repression				
	0hrs	12hrs	20hrs	28hrs	36hrs
n=100%	38	29	16	7	5
90≤n<100%		3	12	7	1
80≤n<90%		5	5	12	12
70≤n<80%		1	4	6	8
60≤n<70%			1	4	5
50≤n<60%				2	7

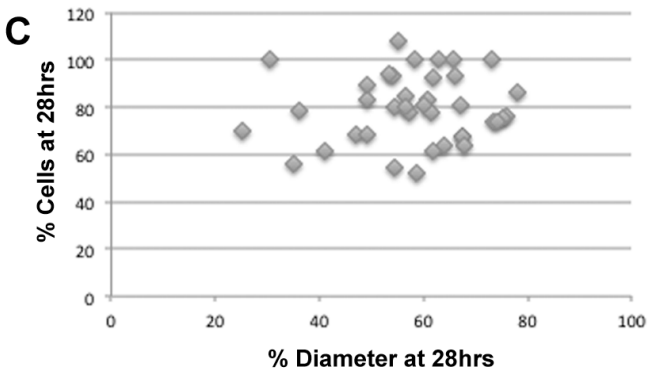

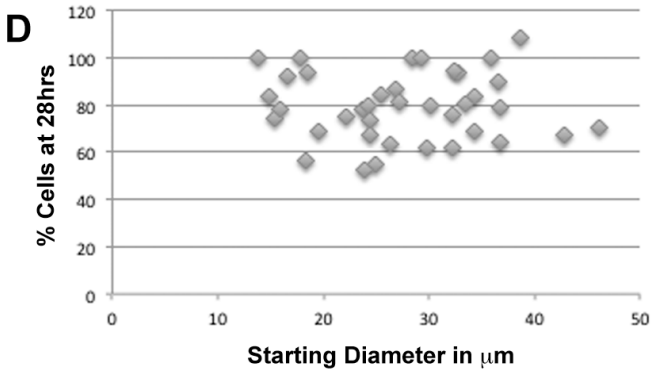

Figure S11. Loss of endothelial cells is not required for AV shunt regression
(A) The table shows the number of AV shunts, over time (columns), binned by the percentage of starting diameter (rows). The bottom panel shows average diameter of all 38 AV shunts and corresponding s.e.m. by percentage of starting diameter. (B) Loss of *TRE-H2B-eGFP* marked cells in AV shunt regression. The table shows the number of AV shunts, over time (columns), binned by the percentage of retained cells (rows). While individual AV shunts displayed variability, initiation of regression by 12hrs usually exhibited no cell loss. Cell number trended downward over time, though many AV shunts retained most or all of their GFP+ endothelial cells. (C) There was no apparent correlation between the percentage of cell loss and the degree of shunt regression by 28hrs. (D) There was no apparent correlation between the percentage of cell loss by 28 hours and the starting AV shunt diameter.

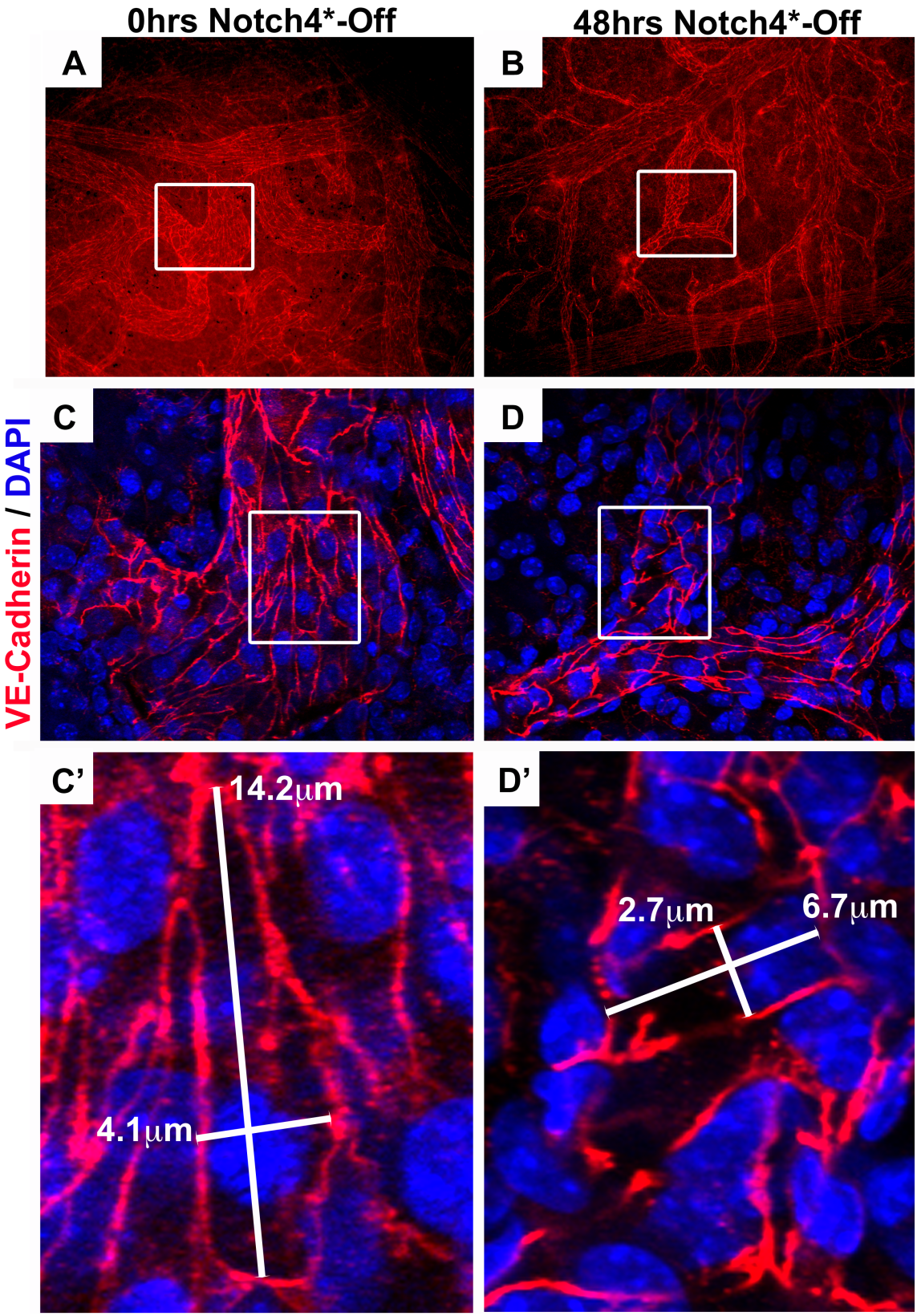

Figure S12. Endothelial cells are narrowed in regressing AV shunts

(A-D) Fluorescent immunostaining of VE-cadherin in *Notch4** mutant mice, imaged in whole mount. Areas shown in A&B were imaged by confocal microscopy at high magnification. Note that the dimensions of endothelial cells were reduced both axially and paraxially along the AV shunt. EC area was reduced (n=4 shunts in one 0hrs *Notch4**-Off mouse: 546μm^2 ± s.d. 193μm) vs. (n=4 shunts in each of two 48hrs *Notch4**-Off mice: 239μm^2 ± s.d. 68μm^2 and 211.4μm^2 ±s.d. 60μm^2).